ELSEVIER

Journal of Hazardous Materials B138 (2006) 142–151

Journal of Hazardous Materials

www.elsevier.com/locate/jhazmat

Adsorption of chromium(VI) on pomace—An olive oil industry waste: Batch and column studies

Emine Malkoc *, Yasar Nuhoglu, Murat Dundar

Department of Environmental Engineering, Faculty of Engineering, Atatürk University, 25240 Erzurum, Turkey

Received 15 December 2005; received in revised form 16 May 2006; accepted 17 May 2006
Available online 26 May 2006

Abstract

The waste pomace of olive oil factory (WPOOF) was tested for its ability to remove chromium(VI) from aqueous solution by batch and column experiments. Various thermodynamic parameters, such as ΔG°, ΔH° and ΔS° have been calculated. The thermodynamics of chromium(VI) ion onto WPOOF system indicates spontaneous and endothermic nature of the process. The ability of WPOOF to adsorb chromium(VI) in a fixed bed column was investigated, as well. The effect of operating parameters such as flow rate and inlet metal ion concentration on the sorption characteristics of WPOOF was investigated. The longest breakthrough time and maximum of Cr(VI) adsorption is obtained at pH 2.0. The total adsorbed quantities, equilibrium uptakes and total removal percents of chromium(VI) related to the effluent volumes were determined by evaluating the breakthrough curves obtained at different flow rates and different inlet chromium(VI) concentrations for adsorbent. The data confirmed that the total amount of sorbed chromium(VI) and equilibrium chromium(VI) uptake decreased with increasing flow rate and increased with increasing inlet chromium(VI) concentration. The Adams–Bohart model were used to analyze the experimental data and the model parameters were evaluated.

Keywords: Adsorption; Pomace (wastes of olive oil factory); Chromium; Fixed bed column; Adams–Bohart model

1. Introduction

The pollution by heavy metals has received wide spread attention in the recent years [1], due to the toxicological importance in the ecosystem, agriculture and human health. Concerning over this problem has led to the development of alternative technologies for effecting the removal of these pollutants from aqueous effluents. The use of low-cost and waste biomaterials as adsorbents of dissolved metal ions has been shown to provide economic solutions to this global problem [2]. In this context, our adsorbent (WPOOF) can be used as an effective and environmentally friendly adsorbent for the treatment of Cr(VI) containing wastewaters.

Chromium is a highly toxic pollutant generated from many industrial processes such as leather tanning processes, electroplating, manufacturing of dye, paint and paper. Chromium exists in the aquatic environment mainly in two states: trivalent Cr(III) and hexavalent Cr(VI). Hexavalent chromium is primarily present in the form of chromate (CrO_2^{4-}) and dichromate (CrO_2^{7-}) ions [3]. The US EPA has set the maximum contaminate level for chromium in drinking water at 0.1 mg L^{-1}. These standards are based on the total concentration of the trivalent and hexavalent forms of dissolved chromium. Chromium has the potential to cause the following health effects from long-term exposures at levels above the MCL: damage to liver, kidney circulatory and nerve tissues; dermatitis. Furthermore, chromium has serious effects on the health of human being [4].

Conventional methods for removing dissolved heavy metal ions include chemical precipitation, chemical oxidation and reduction, ion exchange, filtration, electrochemical treatment and evaporative recovery. However, these high-technology processes have significant disadvantages, including incomplete metal removal, requirements for expensive equipment and monitoring systems, high reagent or energy requirements or generation of toxic sludge or other waste products that require disposal [5].

Adsorption on activated carbon has been found to be an effective process for Cr(VI) removal, but it is too expensive. Natural materials that are available in large quantities, or certain waste products from industrial or agricultural operations, may have

* Corresponding author. Fax: +90 442 2360957.
E-mail address: emalkoc@atauni.edu.tr (E. Malkoc).

0304-3894/$ – see front matter © 2006 Elsevier B.V. All rights reserved.
doi:10.1016/j.jhazmat.2006.05.051

potential as inexpensive sorbents. Due to their low cost, after these materials have been expended, they can be disposed of without expensive regeneration. Most of the low cost sorbents have the limitation of low sorptive capacity and thereby for the same degree of treatment, it generates more solid waste (pollutant laden sorbent after treatment), which poses disposal problems. Therefore, there is need to explore low cost sorbent as our biosorbent (WPOOF) having high contaminant sorption capacity [6]. Consequently numerous low cost alternatives have been studied including Beech sawdust [7], eucalyptus bark [8], green algae (*Ulothrix zonata*) [9], seaweeds [10], coirpith [11], peanut husks carbon [12], zeolite tuff [13], activated carbon derived from agricultural waste material and activated carbon fabric cloth [14], bagasse fly ash [15], activated slag [16], etc. New economical, easily available and highly effective adsorbents are still needed. Generally, biosorptive processes can reduce capital costs by 20%, operational costs by 36% and total treatment costs by 28%, compared with the conventional systems [17].

A thorough literature survey indicated that pomace waste of olive oil factory has not been used as adsorbent for remove of chromium thus far. The objectives of the present study is to adsorb Cr(VI) from aqueous solution by pomace of olive oil mill using batch and fixed-bed column. In batch studies, the dynamic behavior of the adsorption was investigated on the effect of initial metal ion concentration, temperature, adsorbent mass and pH. The thermodynamic parameters were also evaluated from the adsorption measurements. The Langmuir, Freundlich were used to fit the equilibrium isotherm. The important design parameters such as flow rate of fluid and initial concentration of metal solution have been investigated. The breakthrough curves for the adsorption of metals were analyzed using Adams–Bohart model.

2. Material and methods

2.1. Adsorbent

The waste pomace of olive oil factory (WPOOF) (Turkish: prina) is an oil-cake produced by the olive oil mill in Mediterranean countries. It is a solid residue after pressing the olive. This residue includes olive (6–8%), water (20–33%), seeds and pulps (59–74%) depending on the olive oil extraction processes. Prina is used not only soap producing, but also combustible matter to remove water from it. The olive oil mills generate about 15–22 kg olive oil and 35–45 kg prina from 100 kg olive depending on olive quality, olive oil extraction processes and environmental conditions [18]. The prina was obtained from olive oil mill located in Aegean region in Manisa, Turkey. It was washed with distilled water many times and dried at room temperature. Then it was grinded with strong grinder, and sieved to obtain the desired particle size (1.0–3.3, 0.15–0.25 mm). The adsorbent dose was varied between 5.0 and 15 g L^{-1}. The physical characteristic of WPOOF is presented in Table 1.

2.2. Analysis of chromium(VI) ions

The concentration of *residual* chromium(VI) ions in the effluent was *read* spectrophotometrically (Beckman DU 530 UV–vis spectrophotometer) by using diphenyl carbazide as the complexing agent. One milliliter of a 0.2% (w/v) of diphenyl carbazide solution prepared in 95% ethyl alcohol and 1 mL of 1/5 H_2SO_4 solution was added to the sample (1 mL) containing less than 100 mg L^{-1} of chromium(VI) ions and diluted to 100 mL with double-distilled water. The absorbance of the purple colored solution was read at 540 nm after 10 min [5,19].

Table 1
Physical properties of WPOOF used in the experiments

Physical characteristics	Units	Specifications
Particle size (mm)	0.15–0.25 1.00–3.00	Batch studies Column studies
Bulk density (g cm^{-3})	0.509 0.748	Particle size: 0.15–0.25 mm Particle size: 1.00–3.00 mm
BET surface area (m^2 g^{-1})	1.24	Particle size: 0.15–0.25 mm

2.3. Batch studies

The stock solution of Cr(VI) was made by dissolving 2.828 g $K_2Cr_2O_7$ in 1 L double distilled water which was contained 1 g L^{-1} of chromium(VI) ion. Experiments were conducted in 250 mL Erlenmeyer flasks containing known Cr(VI) synthetic solutions. Flasks were agitated on a shaker at 6 rps constant shaking rate for 180 min to ensure equilibrium was reached and filtered through (Schleicher&Schüll589). Samples (5 mL) were taken before mixing the adsorbent solution and Cr(VI) ion bearing solution and at pre-determined time intervals (1, 5, 10, 20, 30, 60, 120 and 180 min) for the residual Cr(VI) ion concentration in the solution. Adsorption experiments were carried out 0.15–0.25 mm at adsorbent particle size. The pH of each test solution was adjusted to the required value with diluted and concentrated H_2SO_4 and NaOH solutions. The zeta potential of waste pomace of olive oil factory (WPOOF) was measured with a Zeta-Meter (ZETAMETER 3:0/542, USA).

2.4. Column studies

The fixed-bed columns were made of Perspex tubes 2.0 cm internal diameter and 30 cm in height. The bed length used in the experiments was 10 cm. In a typical experiment the metal of a known concentration was pumped at a fixed flow rate to the filled with known bed height of adsorbent. The particle size of adsorbent used in the experiment was 1.0–3.0 mm. The pH of the solutions was maintained constant at 2.0. The temperature of stream feeding solution and of the column was controlled at 25 °C through a thermostatic bath. The bed porosity was 0.20.

3. Result and discussions

3.1. Characterization of the adsorbent

Characterization of the adsorbent was investigated by FT-IR spectral and scanning electron microscopy (SEM) investigations.

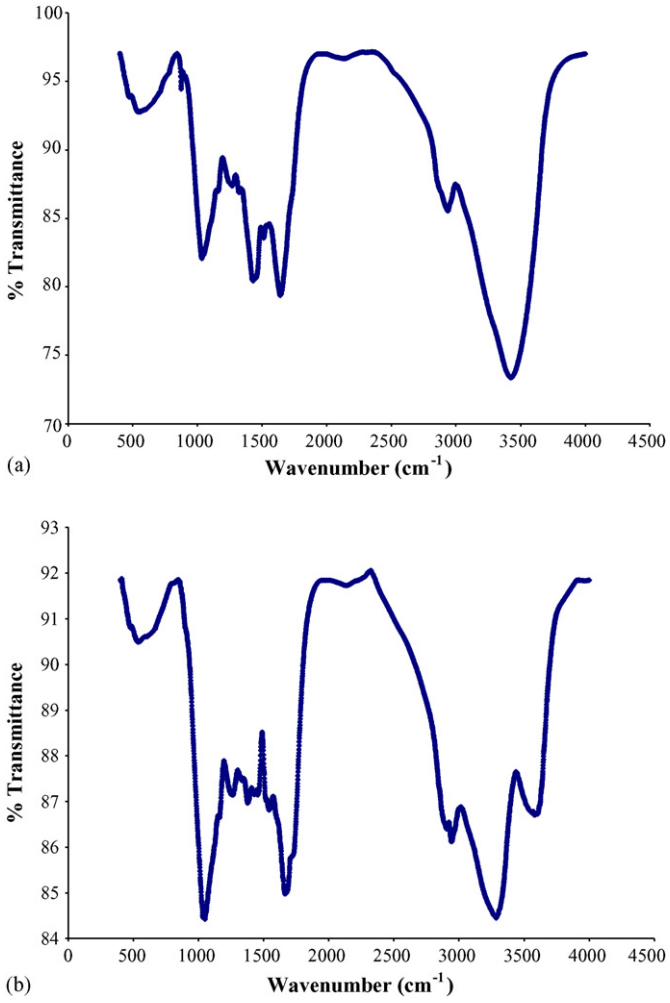

Fig. 1. (a) The FT-IR spectra of WPOOF before adsorption. (b) The FT-IR spectra of WPOOF after adsorption.

3.1.1. Fourier transform infrared spectroscopy (FT-IR) investigations

The FT-IR spectra before and after adsorption of WPOOF are shown in Fig. 1a and b. The functional groups before and after adsorption on WPOOF and the corresponding infrared absorption *bands* are shown in Table 2.

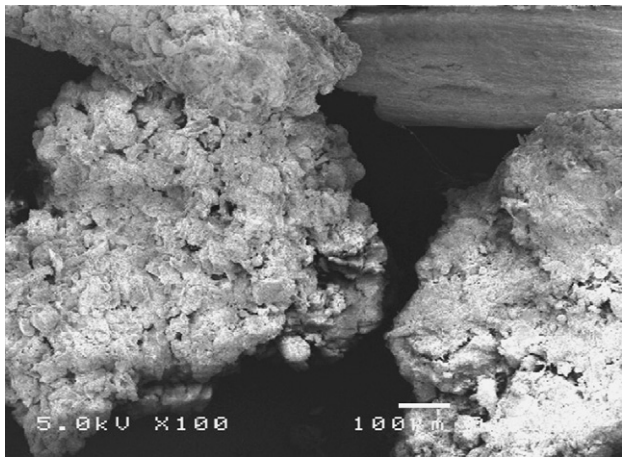

Fig. 2. SEM micrograph of the particles of WPOOF before Cr(VI) adsorption (100×).

As shown in Fig. 1a and b and Table 2, the spectra display a number of absorption peaks, indicating the complex nature of WPOOF. These band shifts indicated that especially the bonded –OH groups and/or –NH stretching and carboxyl groups were especially played a major role in chromium(VI) biosorption on WPOOF [2,20,21].

3.1.2. Scanning electron microscopy of WPOOF

Scanning electron microscopy (SEM) of material used was carried out in a JEOL JSM T-330 unit. In order to see the surfaces of particles after and before adsorption, SEM analysis for the samples of the raw and treated adsorbents were performed from the raw and treated adsorbents (Figs. 2 and 3). It is clearly seen the surfaces of particles after adsorption in Fig. 3 that, the pores and surfaces of adsorbent were covered and became smooth by adsorbate.

3.2. Batch studies

3.2.1. Effect of initial pH

Aqueous phase pH governs the speciation of metals and also the dissociation of active functional sites on the sorbent. It is seen the FT-IR spectra that carboxyl groups display strong peaks at the ranges of 1421 cm^{-1}. The carboxyl functional groups play

Table 2
The FT-IR spectral characteristics of WPOOF before and after adsorption

IR peak	Absorption bands (cm^{-1})			Assignment
	Before adsorption	After adsorption	Differences	
1	3406	3274	−132	Bonded –OH groups, –NH stretching
2	2928	2936	+8	Aliphatic C–H group
3	1635	1662	+27	C=O stretching
4	1507	1536	+29	Secondary amine group
5	1421	1372	−49	Carboxyl groups
6	1317	1320	+3	Symmetric bending of CH_3
7	1243	1243	0	$–SO_3$ stretching
8	1140	1144	+4	C–O stretching of ether groups
9	1029	1031	+2	–C–C– group
10	873	895	+22	–C–C– group

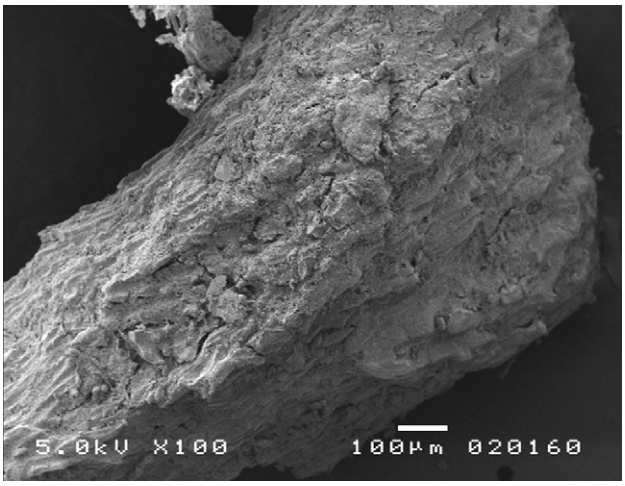

Fig. 3. SEM micrograph of the particles of WPOOF after Cr(VI) adsorption (100×).

a major role in the uptake of the metal cations [2]. Hence, metal sorption is critically linked with pH. Not only different metals show different optimum pH for their sorption but may also vary from one kind of biomass to the other [22].

The effect of pH on the removal of Cr(VI) is investigated by testing four values of pH 2.0, 3.0, 4.0 and 5.0 at a temperature of 25 ± 1 °C. The contact time has been fixed to 180 min for all the experiments. The experimental results are presented in Fig. 4. From Fig. 4 it was observed that the maximum adsorption occurred at pH 2.0. The sorption capacity of Cr(VI) at pH 2.0 by WPOOF was 8.4 mg g^{-1}, which reduced to 2.7 mg g^{-1} at pH 5.0.

The electrical potential at the surface of a particle is zeta potential. It can be determined by the measurement of the velocity of particles in the electric field. At 3.0, 4.0, 5.0, 6.0 and 7.0 the zeta potentials of WPOOF were −19.8, −26, −25.4, −25.2 and −25 mV, respectively. The zeta potential values could not be measured due to the high ionic strength at pH 1.0–2.0, but it was considered that these values were slightly positive. At low pH, there is presence of a large number of H^+ ions, which in turn neutralize the negatively charged adsorbent surface thereby reducing hindrance to the diffusion of dichromate

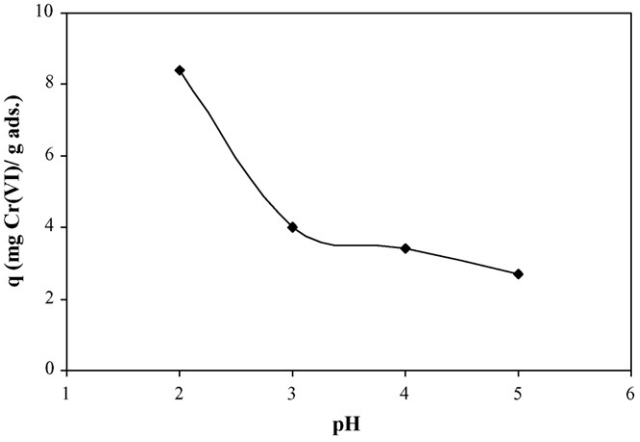

Fig. 4. Effect of pH for the concentration of 100 mg L^{-1}.

ions [1]. Hence, the sorption increases with the increase in the acidity of the solution. But as the pH rises, the concentration of OH^- ions increases and overall charge on the sorbent surface becomes negative which causes hindrance in the sorption of negatively charged Cr ions like $Cr_2O_7^{2-}$, CrO_4^{2-}, etc., results in the decreased sorption of Cr(VI) at higher pH [23].

Many studies have claimed that Cr(VI) was removed from the aqueous phase through an adsorption mechanism, whereby anionic Cr(VI) ion species bind to the positively charged groups of nonliving biomass [7,9,24]. It has been explained that Cr(VI) was completely reduced to Cr(III) by contact with biomass [2,24,25]. Based on the present investigations, the following mechanism of Cr(VI) removal by nonliving biomass is proposed [2,24]. Cr(VI) can be removed from the aqueous phase by nonliving biomass through two mechanisms. In mechanism I (direct reduction), Cr(VI) is directly reduced to Cr(III) in the aqueous phase by contact with the electron-donor groups of the biomass, i.e. groups having lower reduction potential values than that of Cr(VI). Mechanism II (indirect reduction); however, consists of three steps: (1) the binding of anionic Cr(VI) ion species to the positively charged groups present on the biomass surface, (2) the reduction of Cr(VI) to Cr(III) by adjacent electron-donor groups, and (3) the release of the Cr(III) ions into the aqueous phase due to electronic repulsion between the positively charged groups and the Cr(III) ions, or the complexation of the Cr(III) with adjacent groups capable of Cr-binding [2]. Amino and carboxyl groups take part in reaction 1 in mechanism II. As the pH of the aqueous phase is lowered, the large number of hydrogen ions can easily coordinate with the amino and carboxyl groups present on the biomass surface. Thus, low pH makes the biomass surface more positive. The more positive the surface charge of the biomass, the faster the removal rate of Cr(VI) in the aqueous phase, since the binding of anionic Cr(VI) ion species with the positively charged groups is enhanced [2,9]. The low pH also accelerates the reduction reaction in both mechanisms I and II, since the protons take part in this reaction. The solution pH is the most important controlling parameter in the practical use of nonliving biomass in the adsorption process [26]. Hence, it is of significance that the pH of wastewaters containing heavy metals is generally very acidic. Meanwhile, if there are a small number of electron-donor groups in the biomass or protons in the aqueous phase, the chromium bound to the biomass can remain in the hexavalent state. Therefore, a portion of mechanisms I and II depend on the biosorption system (solution pH, temperature, species on the biomass, and biomass and Cr(VI) concentrations) [2].

3.2.2. *Effect of adsorbent dosage*

The removal of chromium by WPOOF at different adsorbent doses (5–15 g L^{-1}) for the chromium concentration 100 mg L^{-1} is investigated. The results are shown that the percent removal of Cr(VI) increases rapidly with increase in the dose of WPOOF due to the greater availability of the adsorbent [27]. The increase in adsorbent dosage from 5.0 to 15 g L^{-1} resulted in an increase from 51.7 to 98.6% in adsorption of Cr(VI) ions. However, uptake of Cr(VI) showed a reverse trend to the removal percentage adsorptions. With increasing adsorbent dosage from 5.0 to

Table 3
The equilibrium uptake capacities and adsorption yields obtained at different initial concentrations and temperatures

C_0 (mg L^{-1})	25 °C		45 °C		60 °C	
	q (mg g^{-1})	% adsorption	q (mg g^{-1})	% adsorption	q (mg g^{-1})	% adsorption
50	6.10	61.00	8.17	81.74	10.00	100.0
100	10.34	51.70	10.88	54.40	12.92	64.60
150	10.80	36.00	12.53	41.77	14.46	48.20
200	2.15	30.37	13.02	32.55	16.49	41.22

Table 4
Freundlich and Langmuir isotherms constants of Cr(VI) adsorption on WPOOF at different temperature

T (°C)	ΔG° (kJ mol^{-1})	Langmuir constants		Freundlich constants	
		Q_0 (mg g^{-1})	b (L mg^{-1})	K_f	n
25	−2.06	13.95	0.0442	2.45	3.00
45	−0.88	14.07	0.0465	3.60	3.95
60	−0.21	18.69	0.0554	6.41	5.16

15 g L^{-1}, the adsorption of Cr(VI) ion per unit weight of adsorbent decreased from 10.34 to 6.57 mg g^{-1}.

3.2.3. Effect of initial Cr(VI) concentration on temperature dependent adsorption

In Table 3, at 25 °C, when the initial Cr(VI) ion concentration increased from 50 to 200 mg L^{-1}, Cr(VI) adsorption removal decreased from 61% to 30.37% and the uptake capacity of WPOOF increased from 6.1 to 12.15 mg g^{-1}. At 25 °C for a Cr(VI) concentration of 50 mg L^{-1} after a 180 min of sorption time, while chromium concentration was measured as 19.7 mg L^{-1}, for 60 °C no chromium was remained. This is also in line with the equilibrium uptake capacity at higher solute concentration. The increase in uptake capacity of pomace with the increase of Cr(VI) ion concentration is due to higher availability of Cr(VI) ions in the solution, for the adsorption. Moreover, higher initial Cr(VI) concentration increased driving force to overcome all mass transfer resistance of metal ions between the aqueous and solid phases resulting in higher probability of collision between Cr(VI) ions and sorbents. This also results in higher metal uptake [23].

Table 3 shows that, the equilibrium uptake capacity of WPOOF increased with increasing initial Cr(VI) concentration up to 200 mg L^{-1} because the initial Cr(VI) concentration provided an important driving force to overcome all mass transfer resistance. The increases of loading capacity of WPOOF with increasing initial Cr(VI) concentration may also be due to higher interaction between metal ion and adsorbent. As WPOOF offered a finite number of surface binding sites, Cr(VI) adsorption showed a saturation trend at higher initial Cr(VI) concentration. Also, the rise in sorption capacity with temperature is because of rise in the kinetic energy of sorbent particles. Thus, the collision frequency between sorbent and sorbate increases; which results in the enhanced sorption on to the surface of the sorbent. Secondly, at high temperature due to bond rupture of functional groups on adsorbent surface there may be an increase in number of active sorption sites, which may also lead to enhanced sorption with the rise in temperature [23].

Table 5
Characteristics of adsorption Langmuir isotherms

Separation factor, R_L	Characteristics of adsorption Langmuir isotherms
$R_L > 1$	Unfavorable
$R_L = 1$	Linear
$0 < R_L < 1$	Favorable
$R_L = 0$	Irreversible

The Langmuir and Freundlich equations were used in the analysis of the adsorption results [28,29]. Q_0, K, K_f, n of Langmuir and Freundlich model constants were determined and presented in Table 3.

The value of correlation coefficient ($R^2 > 0.9905$) indicates that there is a strong positive relationship for the data and that sorption data of the Cr(VI) ion onto WPOOF follows the Langmuir isotherm. The Q_0 for Cr(VI) on WPOOF was increased from 13.95 to 18.69 mg g^{-1} with the increase in temperature from 25 to 60 °C (Table 4). All these results showed that Lang-

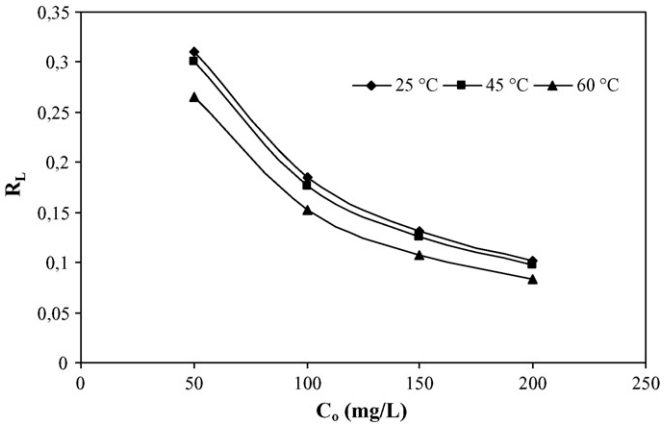

Fig. 5. Separation factor of chromium ions sorbed on different temperatures ($X = 5$ g L^{-1}, pH 2).

Table 6
Comparison of adsorption capacity of other adsorbents for Cr(VI) onto WPOOF

Adsorbent	Adsorption capacity (mg g^{-1})	pH	Max initial Cr(VI) concentration (mg L^{-1})	Reference
Beech sawdust	16.13	1.0	200	[7]
Distillery sludge	5.70	3.0	40	[30]
Sugarcane bagasse	13.40	2.0	500	[31]
Coconut shell carbon	10.88	4.0	25	[32]
Soya cake	0.28	1.0	34.25	[33]
Iron(III) hydroxide-loaded sugar beet pulp	5.12	4.4	200	[34]
HSAC	17.70	2.0	30	[35]
Olive oil factory wastes	12.15	2.0	200	This work

muir isotherm model fitted the results quite well suggesting that the surface of the sorbent is homogenous. Each binding site accepts only one Cr(VI) molecule, that sorbed molecules are organized as a monolayer and all sites are energetically equivalent and there is no interaction between sorbed molecules [23].

The Langmuir parameters can be used to predict the affinity between the sorbate and sorbent using the dimensionless separation factor (R_L) and the criteria shown in Table 5.

As seen Fig. 5, the values of R_L for adsorption of Cr(VI) on WPOOF at studied different concenrations and temperatures were between 0 and 1, which indicates favorable adsorption of Cr(VI) on waste pomace of olive oil factory.

Values of adsorption capacity of the other adsorbents are given in Table 6 for comparison.

Thermodynamic parameters such as change in free energy (ΔG°), enthalpy (ΔH°) and entropy (ΔS°) were determined using the following equations.

The apparent equilibrium constant (K_C) of the biosorption is defined as

$$K_C = \frac{C_{ad,eq}}{C_{eq}} \quad (1)$$

where $C_{ad,eq}$ and C_{eq} is the concentration of Cr(VI) on the adsorbent and residual Cr(VI) concentration at equilibrium, respectively. In this case the activity should be used instead of concentration in order to obtain the standard thermodynamic equilibrium constant (K_C) of the adsorption system [36]

$$\Delta G^\circ = -RT \ln K_C \quad (2)$$

where ΔG° is standard free energy change, J; R the universal gas constant, 8.314 J mol^{-1} K^{-1} and the absolute temperature, K [37]

$$\ln K_C = -\frac{\Delta G}{RT} = -\frac{\Delta H}{RT} + \frac{\Delta S}{R} \quad (3)$$

The plot of $\ln K_C$ as a function of $1/T$ yields (Fig. 6) a straight line from which ΔH° and ΔS° can be calculated from the slope and intercept, respectively. The thermodynamic parameters Gibbs free energy change, ΔG°, are shown in Table 4. The enthalpy change, ΔH°, and the entropy change, ΔS°, for the sorption processes are calculated to be 11.84 and 34.80 J mol^{-1} K^{-1}, respectively. Thermodynamic constants were also evaluated using equilibrium constants changing with temperature. Positive value of ΔH° indicates the endothermic nature of adsorbent. ΔG° is negative and decreases further with

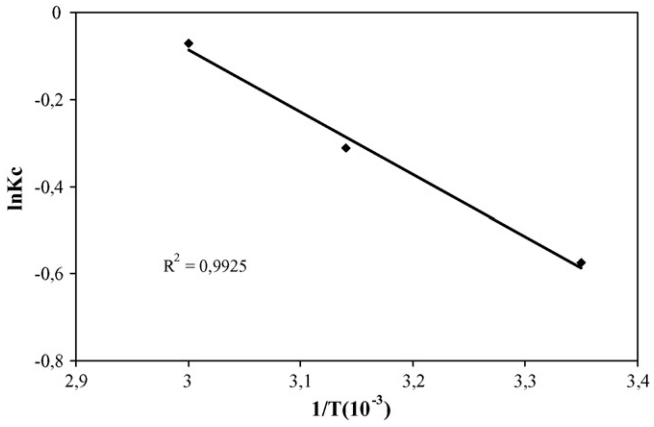

Fig. 6. $\ln K_C$ vs. $1/T$ plot.

increase in temperature indicating that adsorption of Cr(VI) on WPOOF is spontaneous and spontaneity increases with increase in temperature. Positive value of ΔS° suggests randomness at the solid–solution interface during adsorption [38].

3.3. Column studies

3.3.1. Column data analysis

The time for breakthrough appearance and the shape of the breakthrough curve are very important characteristics for determining the operation and the dynamic response of a adsorption column. The breakthrough curves show the loading behavior of metal to be removed from solution in a fixed bed and is usually expressed in terms of adsorbed metal concentration (C_{ad} = inlet metal concentration (C_0) − outlet metal concentration (C_t)) or normalized concentration defined as the ratio of effluent metal concentration to inlet metal concentration (C_t/C_0) as a function of time or volume of effluent for a given bed height [39]. Effluent volume (V_{eff}) can be calculated from the following equation:

$$V_{eff} = Qt \quad (4)$$

where t and Q are the total flow time (min) and volumetric flow rate (mL min^{-1}), respectively. The area under the breakthrough curve (A) obtained by integrating the adsorbed concentration (C_{ad}; mg L^{-1}) versus t (min) plot can be used to find the total adsorbed metal quantity (maximum column capacity). Total adsorbed metal quantity (q_{total}; mg) in the column for a given feed concentration and flow rate is calculated from the following

equation:

$$q_{\text{total}} = \frac{QA}{1000} = \frac{Q}{1000}\int_{t=0}^{t=t_{\text{total}}} C_{\text{ad}}\,\mathrm{d}t \tag{5}$$

Total amount of metal ion sent to column (m_{total}) is calculated from the following equation [40]:

$$m_{\text{total}} = \frac{C_0 Q t_{\text{total}}}{1000} \tag{6}$$

Total removal is calculated from the following equation [39]:

$$\text{Total removal}(\%) = \frac{q_{\text{total}}}{m_{\text{total}}} \times 100 \tag{7}$$

Equilibrium metal uptake (q_{eq}) (or maximum capacity of the column) in the column is defined by Eq. (8) as the total amount of metal sorbed (q_{total}) per gram of sorbent (X) at the end of total flow time [39]

$$q_{\text{eq}} = \frac{q_{\text{total}}}{X} \tag{8}$$

The breakthrough is usually defined as the phenomenon when the effluent concentration from the column is about 3–5% of the influent concentration [41,42]. The number of bed volumes (BV) is defined as

$$\text{number of bed volumes} = \frac{\text{volume of solution treated}}{\text{volume of adsorption bed}} = \frac{\text{operating time}}{\text{EBRT}} \tag{9}$$

The empty bed residence time EBRT is the time required for the liquid to fill the empty column [43]

$$\text{EBRT} = \frac{\text{bed volume}}{\text{volumetric flow rate of the liquid}} \tag{10}$$

The adsorbent exhaustion rate is the mass of adsorbent used per volume of liquid treated at breakthrough [43]

$$\text{adsorbent exhaustion rate} = \frac{\text{mass of adsorbent in column}}{\text{volume treated at breakthrough}} \tag{11}$$

3.3.2. *Effect of flow rate*

The breakthrough curves of Cr(VI) adsorption by WPOOF at different flow rates (5–20 mL min^{-1}) and at fixed bed height of 10 cm are shown in Fig. 7. An earlier breakthrough and exhaustion time were observed in the profile, when the flow rate was increased to 20 mL min^{-1}. The flow rate also strongly influenced the Cr(VI) uptake capacity of as 3.33, 1.17 and 0.96 mg g^{-1}, which were recorded at 5, 10 and 20 mL min^{-1}, respectively.

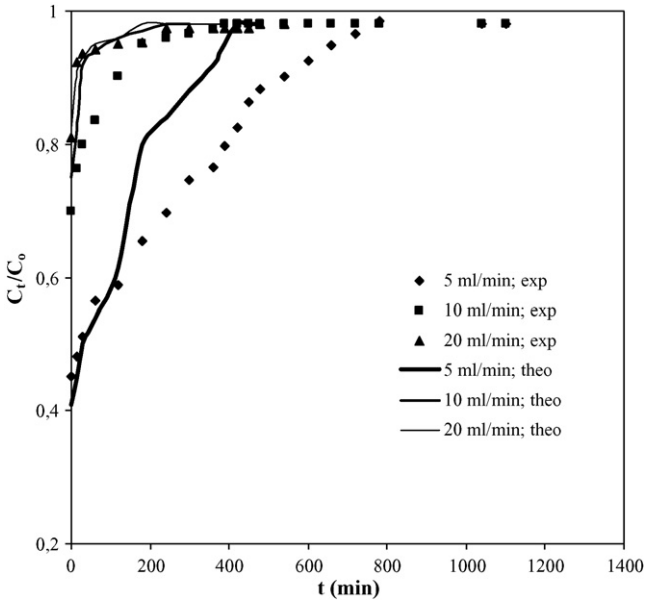

Fig. 7. Comparison of the experimental and predicted breakthrough curves obtained at different flow rates according to the Adams-Bohart model (C_0 = 100 mg L^{-1}, pH of the solution = 2.0, particle size = 1.0–3.0 mm, bed height = 10 cm).

The breakthrough curve becomes steeper when the flow rate is increased with which the break point time and adsorbed Cr(VI) ion concentration decreases. The probable reason behind this is that when the residence time of the solute in the column is not long enough for adsorption equilibrium to be reached at that flow rate, the Cr(VI) solution leaves the column before equilibrium occurs [28]. Thus, the contact time of metal ions with WPOOF is very short at higher flow rate, causing a reduction in removal efficiency.

Accordingly, the breakthrough takes place at 124, 57.3, 38.2 BV for flow rate 5, 10 and 20 mL min^{-1}, respectively; the respective empty bed residence time (EBRT) are 6.28, 3.14 and 1.57 min. Comparison of these values indicates that the treated bed volume (BV) increases with a higher EBRT. In other words, with a higher EBRT, Cr(VI) ions had more time to contact with WPOOF, which resulted in higher removal of Cr(VI) ions in fixed-bed columns [44]. While adsorbent exhaustion rate was

Table 7
The effect of flow rate and initial Cr(VI) concentration on the total adsorbed quantity of Cr(VI) (q_{total}), equilibrium Cr(VI) uptake (q_{eq}) and total removal percentage of Cr(VI) for adsorption to Cr(VI) onto WPOOF

Q (mL min^{-1})	C_0 (mg L^{-1})	t_{total} (min)	m_{total} (mg)	q_{total} (mg)	q_{eq} (mg g^{-1})	Total metal removal (%)
5	100	780	360	78.26	3.33	21.74
10	100	390	390	27.15	1.17	6.96
20	100	240	480	22.46	0.96	4.68
10	50	420	210	23.13	0.98	11.01
10	75	360	270	24.98	1.06	6.90
10	200	240	480	34.65	1.47	7.22

6.02 g L^{-1} at 5 mL min^{-1} flow rate, adsorbent exhaustion rate obtained at 20 mL min^{-1} flow rate was increased 39.2 g L^{-1}.

The sorption data were evaluated and the total sorbed quantities, maximum Cr(VI) uptakes and removal percents with respect to flow rate are presented in Table 7. As seen Table 7, in general the total sorbed Cr(VI) quantity, maximum Cr(VI) uptake and Cr(VI) removal percentage values decreased with increasing flow rate. Furthermore, maximum values of total sorbed Cr(VI) quantity, maximum Cr(VI) uptake and Cr(VI) removal percentage were obtained as 78.26 mg, 3.33 mg g^{-1} and 21.74%, respectively, at 5 mL min^{-1} flow rate.

Adams–Bohart model based on the surface reaction theory and it assumes that equilibrium is not instantaneous; therefore, the rate of the sorption is proportional to the fraction of sorption capacity still remains on the sorbent [45]. The Adams–Bohart model is used for the description of the initial part of the breakthrough curve [39,46]

$$\ln \frac{C_t}{C_0} = k_{AB} C_0 t - k_{AB} N_0 \frac{Z}{U_0} \quad (12)$$

where C_0 and C_t are the inlet and effluent Cr(VI) concentrations (mg L^{-1}), respectively. Z is the height of the column (cm), U_0 is the superficial velocity (cm min^{-1}), N_0 is saturation concentration in the Adams–Bohart model (mg L^{-1}) and k_{AB} is the mass-transfer coefficient (L mg^{-1} min^{-1}). The range of t should be considered from the beginning to the end of breakthrough. A straight line was attained for this system by plotting $\ln(C_t/C_0)$ against t, which gives the value of k_{AB} from the slope of the line.

The breakthrough curves showed that the superposition of experimental results (points) and the theoretical calculated points (lines) (Figs. 7 and 8). According to Adams–Bohart model, average percentage errors (ε%) calculated [17] according

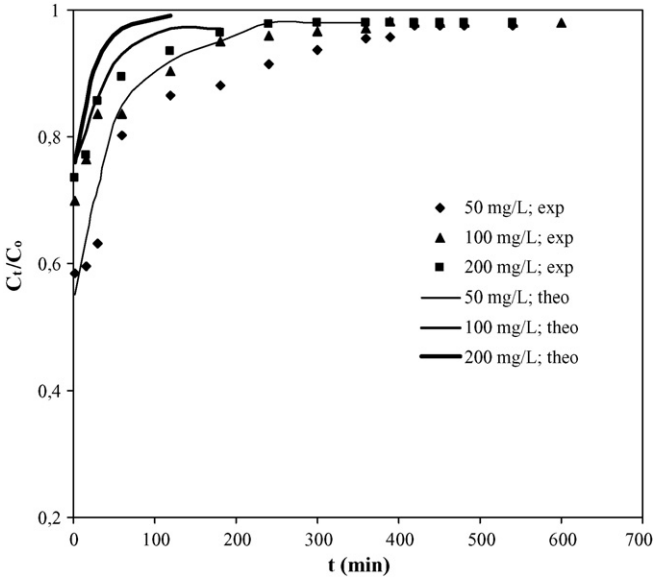

Fig. 8. Comparison of the experimental and predicted breakthrough curves obtained at different inlet Cr(VI) concentration according to the Adams–Bohart model (Q = 10 mL min^{-1}, pH of the solution = 2.0, particle size = 1.0–3.0 mm, bed height = 10 cm).

Table 8
Parameters predicted from the Adams–Bohart models for Cr(VI) adsorption onto waste pomace at different inlet Cr(VI) concentrations and flow rate

C_0 (mg L^{-1})	Q (mL min^{-1})	Adams–Bohart		R^2	ε (%)
		k_{AB} ($\times 10^{-3}$ L mg^{-1} min^{-1})	N_0 (mg L^{-1})		
50	10	0.018	6930	0.7395	4.06
75	10	0.011	9618	0.7796	4.48
100	5	0.004	14568	0.8623	7.79
100	10	0.006	12681	0.7546	2.02
100	20	0.007	9723	0.8814	0.50
200	10	0.0045	15382	0.7379	6.00

to Eq. (13), which indicated the fit between the experimental and predicted values of C_t/C_0 used for plotting breakthrough curves

$$\varepsilon = \frac{\sum_{i=1}^{N} \left[\frac{(C_t/C_0)_{exp} - (C_t/C_0)_{theo}}{(C_t/C_0)_{exp}} \right]}{N} \times 100 \quad (13)$$

N is the number of measurements.

Respective values of N_0 and k_{AB} were calculated from the $\ln(C_t/C_0)$ versus t plots at all flow rates and inlet Cr(VI) concentrations studied are presented in Table 8 together with the correlation coefficients and avarage percentage error. The values of kinetic constant was influenced by flow rate and increased with increasing flow rate. This showed that the overall system kinetics is dominated by external mass transfer in the initial part of adsorption in the column [39].

3.3.3. Effect of feed Cr(VI) concentration

In the sorption of chromium(VI) to WPOOF, a change in inlet chromium(VI) concentration affected the operating characteristics of the fixed bed column. The sorption breakthrough curves obtained by changing inlet chromium(VI) concentration from 50 to 200 mg L^{-1} at 10 mL min^{-1} flow rate and 10 cm bed height are given in Fig. 8. A decreased inlet Cr(VI) concentrations gave delayed breakthrough curves and the treated volume was also higher, since the lower concentration gradient caused slower transport due to decreased diffusion coefficient [40].

At the highest metal concentration (200 mg L^{-1}) the WPOOF bed saturated quickly leading to earlier breakthrough and exhaustion time. Table 7, shows that highest uptake is obtained at the highest metal concentration. It was seen from Table 7, for tested different initial Cr(VI) concentration, maximum bed capacities at 50, 75, 100 and 200 mg L^{-1} Cr(VI) concentration were 0.98, 1.06, 1.17 and 1.47 mg g^{-1}, respectively. The driving force for adsorption is the concentration difference between the Cr(VI) ion on the adsorbent and the metal ion in the solution [39]. Thus the high driving force due to the high metal ion concentration resulted in better column performance.

During the feed solution was sent to the column, upwards of 50% of the inlet Cr^{6+} concentration was exhausted in the initial times (Fig. 8). The 50 mg L^{-1} of Cr^{6+} solutions was exhausted within 360 min (114.6 BV), the 75 mg L^{-1} Cr^{6+} solutions was exhausted within 300 min (95.54 BV), 100 mg L^{-1} Cr^{6+} solutions was exhausted within 180 min (57.3 BV) and 200 mg L^{-1}

Cr^{6+} solutions was exhausted within 120 min (38.2 BV) respectively. The more metal ion concentration was higher, the more adsorbent usage rate was increased and the adsorbent exhaustion rate was higher value. While adsorbent exhaustion rate was 6.53 g L^{-1} at 50 mg L^{-1} Cr^{6+} ion concentration, adsorbent exhaustion rate obtained at 19.58 at 200 mg L^{-1} Cr^{6+} ion concentration.

As expected, maximum adsorption capacity (N_0) increased with increasing inlet Cr(VI) concentration. Predicted and experimental breakthrough curves with respect to flow rate and inlet Cr(VI) concentration are shown in Figs. 7 and 8. It is clear from Figs. 7 and 8 that there was a good agreement between the experimental and predicted normalized concentration values at all Cr(VI) inlet concentrations and flow rates. Thus, developed model and the constants evaluated can be employed for the design of adsorption columns over a range of feasible flow rates and concentrations.

4. Conclusion

The objective of this work was to study the dependence of adsorption on adsorbent and adsorbate (chromium) characteristics by means of both batch and column studies. Conclusions from the present study are as follows:

- The removal of Cr(VI) from aqueous solutions strongly depends on the pH of the solution, adsorbent mass, initial Cr(VI) concentration and temperature. The capacity of adsorption of Cr(VI) increased with increasing temperatures. The maximum adsorption capacity was obtained at pH 2.0. Increase in the mass of the adsorbent leads to increase in Cr(VI) adsorption owing to corresponding increase in the number of adsorption sites.
- The Langmuir and Freundlich adsorption models were used to represent the experimental data fitted very well to the Langmuir isotherm model. The monolayer adsorption capacity (Q^0) was obtained 18.69 mg g^{-1} (optimum pH 2.0, temperature (60 °C), 5 g L^{-1} adsorbent mass and 120 min contact time).
- Thermodynamic calculations showed that the chromium sorption process by waste of olive oil factory has endothermic and spontaneous nature.
- Column studies showed that the adsorption of Cr(VI) onto pomace depends on flow rate and inlet feed Cr(VI) concentration and the data is well fitted by Admas–Bohart model. Comparing the batch and column experiments, batch mode effectively exploited the adsorbent metal binding capacity rather than fixed bed column.
- The employed adsorbent is quite economic than commercially available adsorbents.

Acknowledgement

This research was supported by the Research Project Unit at the Atatürk University under the project no. 2002/147.

References

[1] N. Bishnoi, M. Bajaj, N. Sharma, A. Gupta, Adsorption of Cr(VI) on activated rice husk carbon and activated alumina, Bioresour. Technol. 91 (2004) 305–307.
[2] D. Park, S.-Y. Yun, J.M. Park, Studies on hexavalent chromium biosorption by chemically treated biomass of *Ecklonia* sp., Chemosphere 60 (2005) 1356–1364.
[3] L. Khezami, R. Capart, Removal of chromium(VI) from aqueous solution by activated carbons: Kinetic and equilibrium studies, J. Hazard. Mater. 123 (1–3) (2005) 223–231.
[4] US EPA, National Primary Drinking Water Regulations, Ground Water and Drinking Water, Consumer Factsheet on: CHROMIUM, 1995. Available: http://www.epa.gov/safewater/dwh/t-ioc/chromium.html.
[5] Z. Aksu, F. Gönen, Z. Demircan, Biosorption of chromium(VI) ions by Mowital B30H resin immobilized activated sludge in a packed bed: comparison with granular activated carbon, Process Biochem. 38 (2002) 175–186.
[6] G.S. Agarwal, H.K. Bhuptawat, S. Chaudhari, Biosorption of aqueous chromium(VI) by *Tamarindus indica* seeds, Bioresour. Technol. 97 (2006) 949–956.
[7] F.N. Acar, E. Malkoc, The removal of chromium(VI) from aqueous solutions by *Fagus orientalis* L., Bioresour. Technol. 94 (1) (2004) 13–15.
[8] V. Sarin, K.K. Pant, Removal of chromium from industrial waste by using eucalyptus bark, Bioresour. Technol. 97 (1) (2006) 15–20.
[9] E. Malkoc, Y. Nuhoglu, The Removal of chromium(VI) from synthetic wastewater by *Ulothrix zonata*, Fresen. Environ. Bull. 12 (4) (2003) 376–381.
[10] K. Vijayaraghavan, J. Jegan, K. Palanivelu, M. Velan, Biosorption of cobalt(II) and nickel(II) by seaweeds: batch and column studies, Separ. Purif. Technol. 44 (2005) 53–59.
[11] K. Kadirvelu, K. Thamaraiselvi, C. Namasivayam, Adsorption of nickel(II) from aqueous solution onto activated carbon prepared from coirpith, Separ. Purif. Technol. 24 (2001) 497–505.
[12] S. Ricordel, S. Taha, I. Cisse, G. Dorange, Heavy metals removal by adsorption onto peanut husks carbon: characterization, kinetic study and modeling, Separ. Purif. Technol. 24 (2001) 389–401.
[13] A.A. Al-Haj, R. El-Bishtawi, Removal of lead and nickel ions using zeolite tuff, J. Chem. Tech. Biotechnol. 69 (1997) 27–34.
[14] D. Mohan, K.P. Singh, V.K. Singh, Removal of hexavalent chromium from aqueous solution using low cost activated carbons derived from agricultural waste materials and activated carbon fabric cloth, Indust. Eng. Chem. Res. (ACS) 44 (2005) 1027–1042.
[15] V.K. Gupta, K.T. Park, S. Sharma, D. Mohan, Removal of chromium (VI) from electroplating industry wastewater using bagasse fly ash—a sugar industry waste material, Environmentalist 19 (1999) 129–136.
[16] S.K. Srivastava, V.K. Gupta, D. Mohan, Removal of lead and chromium by activated slag—a blast furnace waste, J. Environ. Eng. (ASCE) 123 (5) (1997) 461–468.
[17] M.X. Loukidou, A.I. Zouboulis, T.D. Karapantsios, K.A. Matis, Equilibrium and kinetic modeling of chromium(VI) biosorption by *Aeromonas caviae*, Colloids Surf. A: Physicochem. Eng. Aspects 242 (2004) 93–104.
[18] E. Malkoc, Removal of Heavy Metals From Waters By Different Adsorbent Types. Ph.D. Thesis, Graduate School of Natural and Applied Sciences, Department of Environmental Engineering, Ataturk University, Turkey, 2005.
[19] E. Malkoc, F.N. Acar, A comparision of adsorption kinetics: Cr(VI) removal from aqueous solutions, Fresen. Environ. Bull. 14 (6) (2005) 509–513.
[20] R.S. Bai, T.E. Abraham, Studies on enhancement of Cr(VI) biosorption by chemically modified biomass of *Rhizopus nigricans*, Water Res. 36 (2002) 1224–1236.
[21] P.X. Sheng, Y.-P. Ting, J.P. Chen, L. Hong, Sorption of lead, copper, cadmium, zinc, and nickel by marine algal biomass: characterization of biosorptive capacity and investigation of mechanisms, J. Colloid Interf. Sci. 275 (2005) 131–141.
[22] D.P. Tiwari, D.K. Singh, D.N. Saksena, Hg (II) adsorption from aqueous solutions using rice–husk ash, J. Environ. Eng. 121 (1995) 479–481.

[23] N. Tewari, P. Vasudevan, B.K. Guha, Study on biosorption of Cr(VI) by *Mucor hiemalis*, Biochem. Eng. J. 23 (2005) 185–192.
[24] D. Park, Y.-S. Yun, J.M. Park, Reduction of hexavalent chromium with the brown seaweed *Ecklonia* biomass, Environ. Sci. Technol. 38 (2004) 4860–4864.
[25] C.P. Huang, M.H. Wu, The removal of chromium(VI) from dilute aqueous solution by activated carbon, Water Res. 11 (1997) 673–679.
[26] Y. Nuhoglu, E. Oguz, Removal of copper(II) from aqueous solutions by biosorption on the cone biomas of *Thuja orientalis*, Process Biochem. 38 (2003) 1627–1631.
[27] D. Mohan, K.P. Singh, V.K. Singh, Trivalent chromium removal from wastewater using low cost activated carbon derived from agricultural waste material and activated carbon fabric cloth, J. Hazard. Mater. B135 (2006) 280–295.
[28] S. Ghorai, K.K. Pant, Equilibrium, kinetics and breakthrough studies for adsorption of fluoride on activated alumina, Separ. Purif. Technol. 42 (2005) 265–271.
[29] A.Y. Dursun, C.S. Kalayci, Equilibrium, kinetic and thermodynamic studies on the adsorption of phenol onto chitin, J. Hazard. Mater. B 123 (2005) 151–157.
[30] K. Selvaraj, S. Manonmani, S. Pattabhi, Removal of hexavalent chromium using distillery sludge, Bioresour. Technol. 89 (2003) 207–211.
[31] D.C. Sharma, C.F. Forster, A preliminary examination into the adsorption of hexavalent chromium using low-cost adsorbents, Bioresour. Technol. 47 (1994) 257–264.
[32] S. Babel, T.A. Kurniawan, Cr(VI) removal from synthetic wastewater using coconut shell charcoal and commercial activated carbon modified with oxidizing agents and/or chitosan, Chemosphere 54 (2000) 951–967.
[33] N. Daneshvar, D. Salari, S. Aber, Chromium adsorption and Cr(VI) reduction to trivalent chromium in aqueous solutions by soya cake, J. Hazard. Mater. B 94 (2002) 49–61.
[34] H.S. Altundogan, Cr(VI) removal from aqueous solution by iron(III) hydroxide-loaded sugar beet pulp, Process Biochem. 40 (2005) 1443–1452.
[35] V.K. Gupta, I. Ali, Removal of lead and chromium from wastewater using bagasse fly ash—a sugar industry waste, J. Colloid Interf. Sci. 271 (2004) 321–328.
[36] E. Malkoc, Y. Nuhoglu, Investigations of nickel(II) removal from aqueous solutions using tea factory waste, J. Hazard. Mater. B127 (2005) 120–128.
[37] J. Romero-Gonzaĭlez, J.R. Peralta-Videa, E. Rodrıĭguez, M. Delgado, J.L. Gardea-Torresdey, Potential of *Agave lechuguilla* biomass for Cr(III) removal from aqueous solutions: Thermodynamic studies, Bioresour. Technol. 97 (1) (2006) 178–182.
[38] M. Ajmal, R.A.K. Rao, R. Ahmad, M.A. Khan, Adsorption studies on *Parthenium hysterophorous* weed: removal and recovery of Cd(II) from wastewater, J. Hazard. Mater. B135 (2006) 242–248.
[39] Z. Aksu, F. Gönen, Biosorption of phenol by immobilized activated sludge in a continuous packed bed: prediction of breakthrough curves, Process Biochem. 39 (2004) 599–613.
[40] T.V.N. Padmesh, K. Vijayaraghavan, G. Sekaran, M. Velan, Batch and column studies on biosorption of acid dyes on fresh water macro alga *Azolla filiculoides*, J. Hazard. Mater. 125 (1–3) (2005) 121–129.
[41] J.P. Chen, X. Wang, Removing copper, zinc, and lead ion by granular activated carbon in pretreated fixed bed columns, Separ. Purif. Technol. 19 (2000) 157–167.
[42] J.P. Chen, J.T. Yoon, S. Yiacoumi, Effects of chemical and physical properties of influent on copper sorption onto activated carbon fixed-bed columns, Carbon 41 (2003) 1635–1644.
[43] D.C.K. Ko, J.F. Porter, G. McKay, Optimised correlations for the fixed-bed adsorption of metal ions on bone char, Chem. Eng. Sci. 55 (2000) 5819–5829.
[44] E. Malkoc, Y. Nuhoglu, Y. Abali, Cr(VI) adsorption by waste acorn of *Quercus ithaburensis* in fixed beds: prediction of breakthrough curves, Chem. Eng. J. 119 (2006) 61–68.
[45] J. Goel, K. Kadirvelu, C. Rajagopal, V. Kumar Garg, Removal of lead(II) by adsorption using treated granular activated carbon: batch and column studies, J. Hazard. Mater. 125 (1–3) (2005) 211–220.
[46] X. Liao, M. Zhang, B. Shi, Collagen-fiber-immobilized tannins and their adsorption of Au(III), Ind. Eng. Chem. Res. 43 (2004) 2222–2227.